frontiers | Frontiers in Remote Sensing

TYPE Original Research
PUBLISHED 09 February 2026
DOI 10.3389/frsen.2025.1572674

OPEN ACCESS

EDITED BY
Alexandre Carmelo Gregory Schimel,
Geological Survey of Norway, Norway

REVIEWED BY
Annalisa Minelli,
Istituto Superiore per la Protezione e la Ricerca Ambientale (ISPRA), Italy
Amy Winsor Nau,
Commonwealth Scientific and Industrial Research Organisation (CSIRO), Australia

*CORRESPONDENCE
Thomas Vandorpe,
thomas.vandorpe@vliz.be

†PRESENT ADDRESSES
Alexia Semeraro,
BLUEGent Innovations in Aquaculture & Blue Life Sciences, GENT, Belgium

RECEIVED 07 February 2025
REVISED 15 December 2025
ACCEPTED 22 December 2025
PUBLISHED 09 February 2026

CITATION
Vandorpe T, Lashkari S, Langedock K, Semeraro A, Van Hoey G, Sterckx T and Moulaert I (2026) Estimating biomass volumes on aquaculture dropper lines using multibeam water column data.
Front. Remote Sens. 6:1572674.
doi: 10.3389/frsen.2025.1572674

Estimating biomass volumes on aquaculture dropper lines using multibeam water column data

Thomas Vandorpe[1]*, Samira Lashkari[1], Kobus Langedock[1], Alexia Semeraro[2†], Gert Van Hoey[2], Tomas Sterckx[3] and Ine Moulaert[1]

[1]Flanders Marine Institute (VLIZ), Oostende, Belgium, [2]Flanders Research Institute for Agriculture, Fisheries and Food (ILVO), Oostende, Belgium, [3]DEME, Zwijndrecht, Belgium

Assessing the biomass on longline setups based on acoustic data hold significant potential for improving the efficiency and accuracy of monitoring and management of aquaculture setups. Traditional assessment methods, such as manual sampling and visual inspections, are not only labor-intensive and time-consuming but are also subject to variability, often leading to under- or overestimations. Acoustic data, particularly multibeam water column (MBWC) data, provide a non-invasive alternative that can significantly enhance biomass estimation. Within this paper, we demonstrate that 2D and 3D visualizations based on MBWC data can effectively display aquaculture longline structures. To facilitate processing of MBWC data, we have developed scripts that allow to filter and cluster the data into individual dropper lines, enabling an estimation of the biomass volume on each dropper line individually. Our approach offers a scalable and cost-effective solution for aquaculture monitoring, reducing the reliance on destructive sampling and improving decision-making capabilities. Future improvements, such as enhanced data density, refined filtering techniques and automated acquisition workflows, will further increase the accuracy and usability of this method. Ultimately, this research provides aquaculture managers with an innovative tool for rapid volume assessments, contributing to the optimization of sustainable aquaculture practices.

KEYWORDS

3D visualization, longline aquaculture, multibeam water column backscatter, python (programming language), volume estimates

1 Introduction

Aquaculture-related production of human food has increased immensely over the past few decades and accounted in 2020 already for more than 50% of the aquatic biomass destined for human consumption (Fao, 2020). For example, the production of marine shellfish and finfish went from 10 million tonnes in 1987 to 122.6 million tonnes in 2020 (Fao, 2022; Naylor et al., 2021). With increasing production comes the need for fast, adequate and performant monitoring techniques, allowing to determine the integrity of the aquaculture setup and the biomass it has produced. Traditionally, mussel aquaculture monitoring has predominantly been conducted manually (Bao et al., 2020), often involving divers (Lowry et al., 2014; Ali et al., 2022), which is labour intensive and inherently contains a certain risk (Peck et al., 2024). These monitoring techniques are also restricted by environmental conditions such as turbidity, currents and waves, leading to limited spatial and temporal coverage. Acoustic methods are increasingly being used in aquaculture

monitoring, mainly in biomass estimates for fish (Li et al., 2024) or to determine the interaction of wild species with cultured species in aquaculture setups (English et al., 2024), but also hold a lot of potential in mussel aquaculture monitoring. One of the main advantages of acoustic methods are their large degree of independence to turbidity and current velocities. Within a bivalve aquaculture longline setup, Brehmer et al. (2003), Brehmer et al. (2006) were the first to use multibeam echosounders to visualize longline setups off the coast of southern France back in 2000 and 2001. However, efforts to refine this method have not been reported since.

Besides seafloor bathymetry and backscatter data, multibeam echosounders are also able to yield backscatter data from the water column, allowing to visualize the water column beneath the transducer. This technique has only been explored for about 35 years, lagging seafloor bathymetric and backscatter research. This is partly due to the large data volumes, recording multibeam water column data (MBWC data) increases the volume of recorded data by a factor 20–100 depending on the data density, and the required processing power, which is much higher compared to seafloor bathymetry and backscatter processing steps. Consequently, very few studies have used MBWC data in the early days (Trenkel et al., 2008). Since the 2010s, an increase in scientific studies focussing on processing of MBWC data and their applications is noticed (Colbo et al., 2014). Examples of applications are gas flare research, where rising bubbles have been detected and quantified using single beam and multibeam echosounders (Urban et al., 2017; Higgs et al., 2019), fisheries, where the ecological behavior of fish school is studied based on the school shapes (Innangi et al., 2016) and suspended particulate matter studies, where suspended sediment concentrations are estimated based on MBWC backscatter information (Fromant et al., 2021; Praet et al., 2023).

Given the lack of sustained efforts to visualize and quantify longlines using multibeam echosounders and the increasing importance of aquaculture in human food production, we intend to use MBWC data acquired from a longline setup to assess the biomass of the organisms on the setup, through volume estimates. Therefore the goals of this paper are to (1) assess if MBWC data can be used to visualize the longline setup in sufficient detail and (2) develop a semi-automated workflow, allowing to cluster individual dropper lines overgrown with bivalves, from MBWC data and estimate their volume.

2 Material and data

Within this study, data from the Coastbusters 2.0 project is used, combined with processing scripts developed within the ULTFARMS project. The initial Coastbusters project (2017–2020) focused on ecosystem-based coastal management and embraced the concept of nature-based solutions (Goedefroo et al., 2022). To achieve long-term coastal resilience, the project developed pioneering steps towards natural biogenic reef development in front of the coast of the Belgian municipality De Panne. Coastbusters 2.0 (2020–2023) investigated the blue mussel biogenic reef concept in two different environments, a sheltered site in between a sandbank (Trapegeer) and the shoreline and a more exposed site seaward of the sandbank (Figures 1A,B; Boulenger et al., 2024). The setup for both sites was

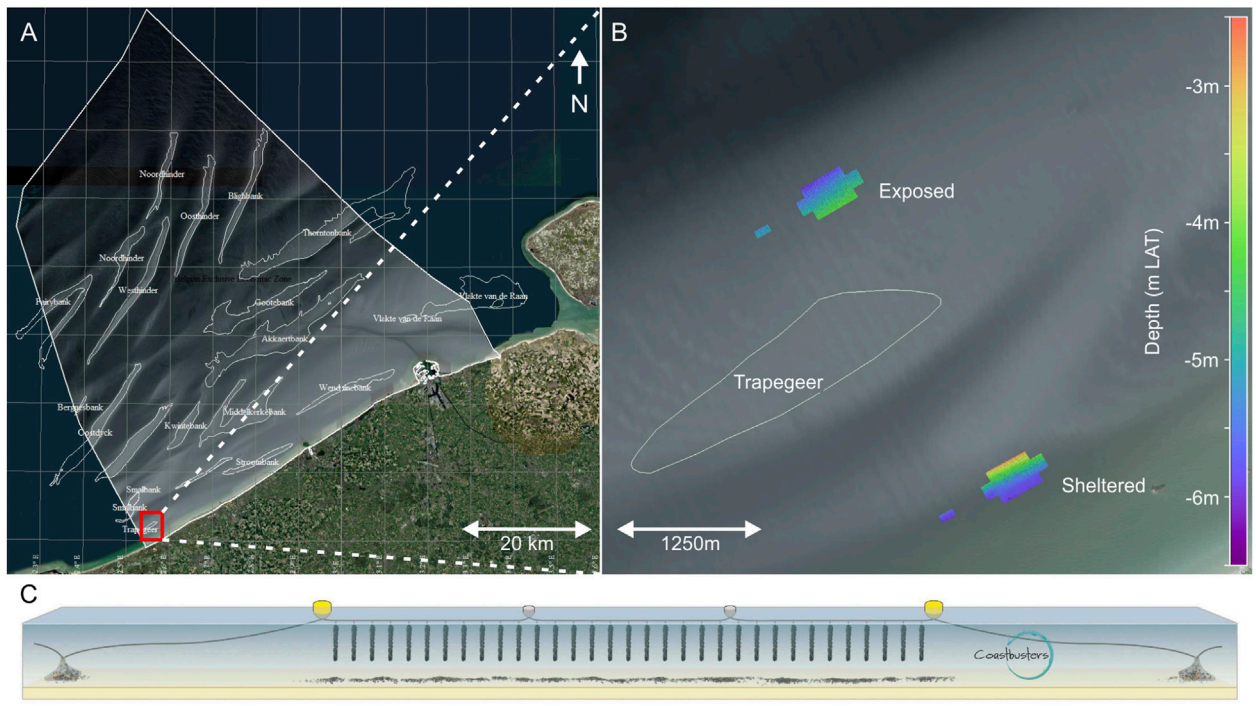

FIGURE 1
(A) Location of the longline systems used in the Coastbusters 2.0 project in the Belgian part of the North Sea. **(B)** Zoom of the research area with indication of the two areas where longlines were installed. The longline used in this study is situated in the sheltered (southern) area. **(C)** Schematic overview of the longline studied within this paper (image: Coastbusters2.0, 2023).

equal and similar to many mussel aquaculture installations consisting of a longline of about 150 m, anchored to the seafloor at both ends and kept afloat using buoys, with thirty-six 3 m long dropper lines attached to it (Figure 1C). The dropper lines are intended for capturing mussel spat and growing the mussels, which eventually become too heavy and drop to the seafloor, forming a mussel reef (Goedefroo et al., 2022). The growth of the mussels on the dropperlines was monitored by seasonal surveys (winter, spring, summer and autumn) where a selection of dropperlines were lifted out of the water, weighed and inspected visually. Additionally, innovative monitoring techniques were tested and assessed as part of the project, including the use of MBWC data for visualizing the setup.

The ULTFARMS project aims at advancing the technology readiness level of low-trophic aquaculture (LTA) within offshore wind farms. To do so, LTA activities are deployed in six offshore wind farms in Belgium, Germany, The Netherlands and Denmark. Within the Belgian pilot, one of the aims is to assess the feasibility of using MBWC data for assessing the biomass of bivalves and to develop a semi-automated processing workflow to estimate their volume. Due to adverse weather conditions during the deployment of the ULTFARMS longline within the Belgian offshore wind farm, no MBWC data could be obtained of the installed longline. As a backup plan, the Coastbusters 2.0 data was used to develop a workflow for volume estimations.

A Norbit WBMS (0.9° across by 1.9° along opening angles) with detachable inertial navigation system (Seabed SBD IMU-S2) and Seabed SGR6-D S2 GNSS positioning system was used to generate the MBWC data on 10 October 2021. The multibeam echosounder was installed over-the-side on the rigid-hulled inflatable boat (RHIB) Zeekat from Flanders Marine Institute (VLIZ; Figure 2). The multibeam echosounder operated at 400 kHz and the opening angle was set at 120° with equidistant spacing of the 512 beams in order to optimally visualize the structures in the water column. The data was acquired using the following settings: a pulse amplitude of 10 (unitless setting), a sweep time of 12 μs and time varied gain parameters as follows: a static gain of −17 dB, a spreading parameter of 40 and 80 dB/km absorption. No absolute calibration of the backscatter intensity values was performed. Given the used multibeam echosounder is not of the most recent generation, increasing the ping rate automatically decreased the inter-sample distance. Therefore, we opted to generate the MBWC data at a pring rate of 15 Hz at the medium resolution setting (categorical parameter within the Norbit WBMS software), yielding a good trade-off between data density in the swath plane and along track ping density of the resulting data. This resulted in an average inter-sample distance of 10.9 cm (202 samples over a 23 m range), while the inter-beam distance varied from 0.41 cm (at 1 m range) to 2.5 cm (at 5 m range). Survey speed during MBWC data acquisition was kept as low as possible, typically around 4 knots (depending on the currents), ensuring the highest along track ping density possible (on average 16.5 cm) while maintaining maneuverability. All data were gathered in a single pass while sailing parallel to the longline system, with an approximate athwartship distance of 1 m between the multibeam echosounder and the longline.

FIGURE 2
RHIB Zeekat (VLIZ) with the portable Norbit echosounder (black), Inertial Navigation System (blue) and GPS system (2 white antennas) installed over-the-side.

Data was acquired with Qinsy (QPS). The raw data were loaded into Qimera (QPS) applying appropriate sound velocity profiles. Qimera contains ping echogram and beamstack profile viewers for MBWC data (either stacked by depth or by range), allowing to get a relatively quick overview of the scatterers within the water column (Figure 3). Qimera displays the water column data in decibels, calculated from the raw intensity values in the 7042-7k compressed water column datagrams, using the 20 * $\log_{10}$ (raw) formula.

During seasonal dropper line inspection surveys in the framework of the Coastbusters 2.0 project, some of the dropper lines were lifted and their circumference at the base and top were measured (Leinung, 2023). The measurements closest to the time of multibeam data acquisition are displayed in Table 1.

3 Methods

3.1 3D visualization

3D visualizations of the aquaculture setup can be valuable to inspect the integrity of the aquaculture setup. While Qimera (QPS) can render a beamstack profile, allowing to view the longline in 2D (Figure 3), 3D displays of the longline alone are not possible with this software. In order to display the longline system in 3D, all unwanted surrounding MBWC data points need to be deleted. However, MBWC data points with the same values as the longline (Figure 3) complicate the automatic detection of aquaculture setups based on simple backscatter value filters. Therefore, manual selection within Qimera (QPS) of longline scatterers has been performed. Since relevant aquaculture scatterers can occur beyond the minimum slant range, where they are affected by sidelobe interference (Hughes Clarke, 2006; Figures 3, 4), and are necessary for a complete 3D visualization of the long- and dropper lines, we opted against filtering out data beyond the minimum slant range for the purpose of 3D visualization. The manually selected MBWC data was exported by Qimera (QPS) into an ascii file containing northing, easting, depth and raw intensity values. This ascii file was loaded into Global Mapper (Blue Marble Geographics), rendering a 3D display of the longline system with the colors indicating the dB values (Figure 5).

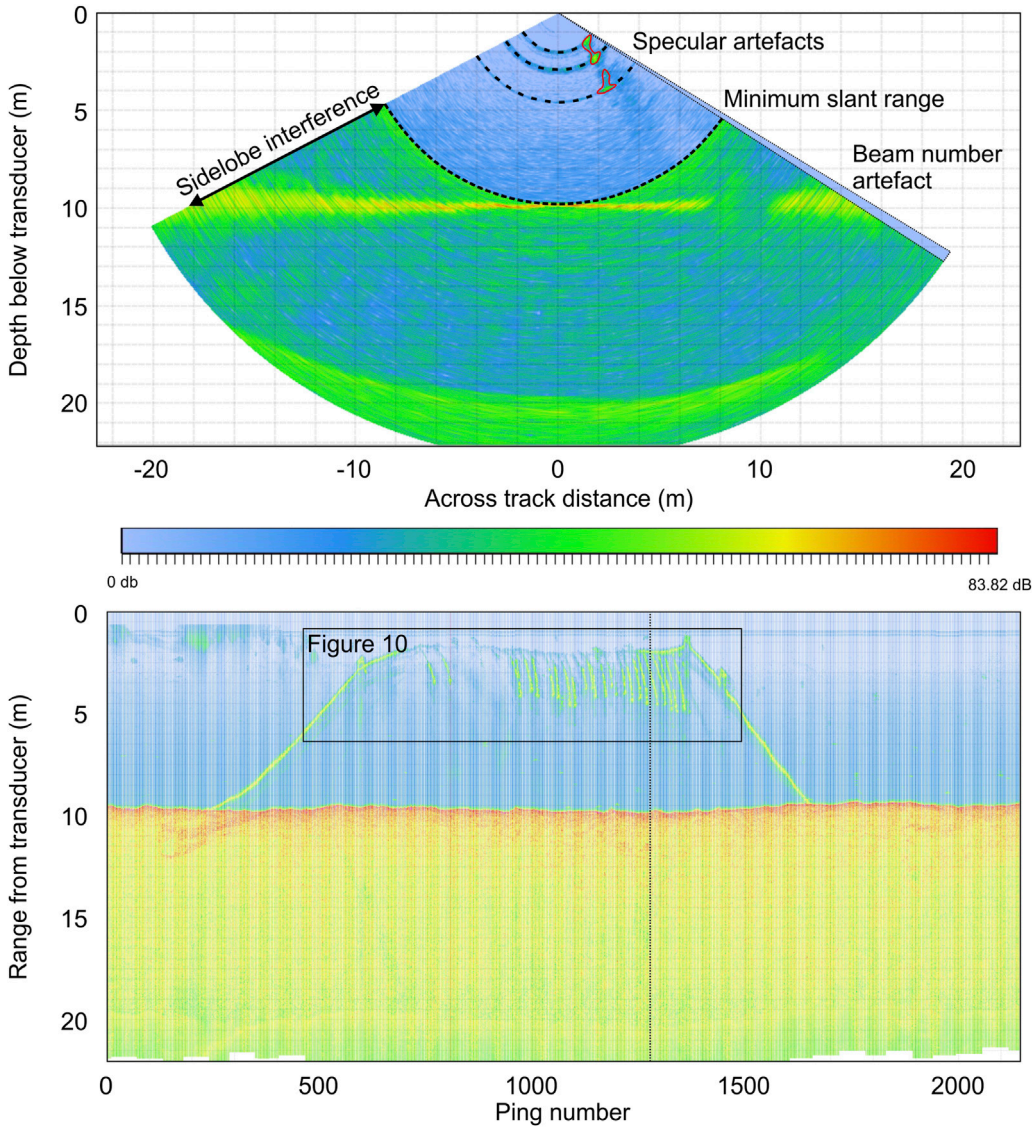

FIGURE 3
MBWC data displayed as a ping echogram (top) and as a beamstack profile stacked by range (bottom). The red lines in the ping echogram indicate the manually selected points. They are accompanied by specular artefacts (Hughes Clarke, 2006). The thin black vertical line in the lower profile indicates the position of the upper ping echogram. The beam number artefact is a thin triangular section on the right hand side of the ping echogram. Both profile are made with Qimera (QPS).

TABLE 1 Dropper line inspection survey data (13/09/2021) of the longline displayed in Figures 3, 10. Dropper line numbers can be seen in Figure 10 and cluster numbers in Figure 8. For more information on the dropper line inspection survey itself, see Leinung (2023).

Dropper line number	Cluster number	Top circumf. (cm)	Base circumf. (cm)
3	absent	37	54
13	20 (entangled)	68	52
25	11	67	59
26	10	48	60
27	absent	59	42
43	3	31	47

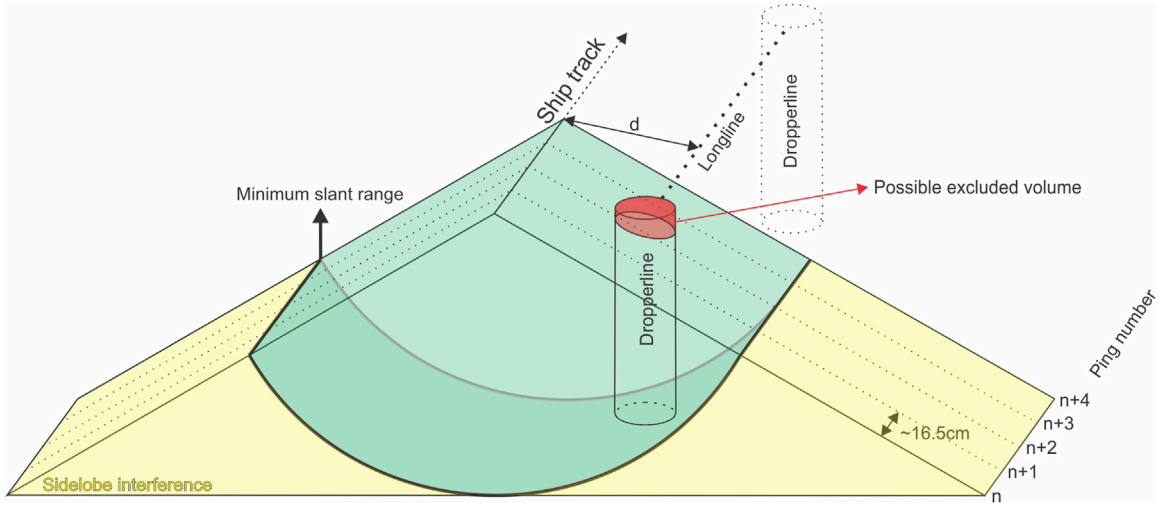

FIGURE 4
3D abstract representation of several pings (n to n+4) of MBWC data. The volume affected by sidelobe interference is indicated in yellow. The green volume is not influenced by sidelobe interference and is used for acoustic volume estimations. The red part of the dropper line, visualized by a cylinder, is posssibly exluded from the MBWC data, depending on the horizontal distance "d" between the multibeam echosounder and the dropper line and the opening angle of the multibeam echosounder.

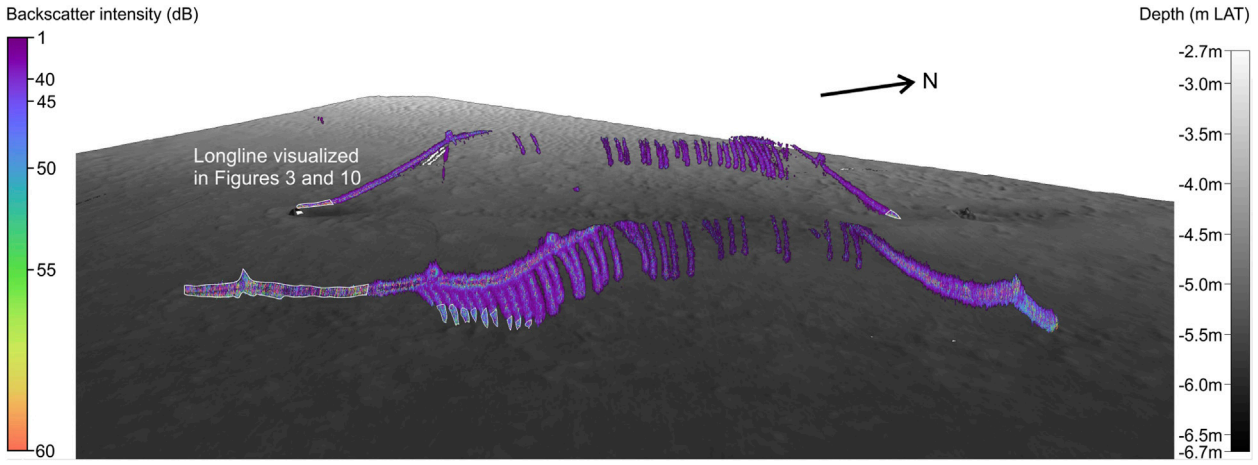

FIGURE 5
3D visualization of the manually selected MBWC point cloud data. The northern longline is used for acoustic volume calculations within this paper and is displayed in the beamstack profile in Figure 3. The parts of the longline surrounded by a thin white line are affected by sidelobe interference and are characterized by higher backscatter intensity values.

3.2 Acoustic volume estimation of individual dropper lines

The workflow described above is solely intended for visualization purposes, is time-consuming and does not allow the selection of individual dropper lines, nor does it allow volume calculations of them. Therefore, purpose-built Python scripts, combined called CloudVolume_multibeam (Lashkari and Vandorpe, 2025), and a graphical user interface (Figure 6) were created. In CloudVolume_multibeam, point cloud data files in ascii format (containing northing, easting, depth, intensity, beam number and ping number) can be loaded. This ascii file was generated by Qimera (QPS), which can export all MBWC data within the minimum slant range (so without manual selection of the relevant data points as described for the 3D visualization). Data beyond the minimum slant range have been discarded as several filtering steps within CloudVolume_multibeam rely on backscatter intensity values (see next section), which are distorted beyond the minimum slant range (Figures 3, 5; Hughes Clarke, 2006; Urban et al., 2017). Note that some parts of the installations, notably those indicated in white in Figure 5, are therefore excluded from the volume calculations. Data from several passes could be loaded at once into CloudVolume_multibeam, providing they are combined into 1 input file. However, since aquaculture setups are prone to

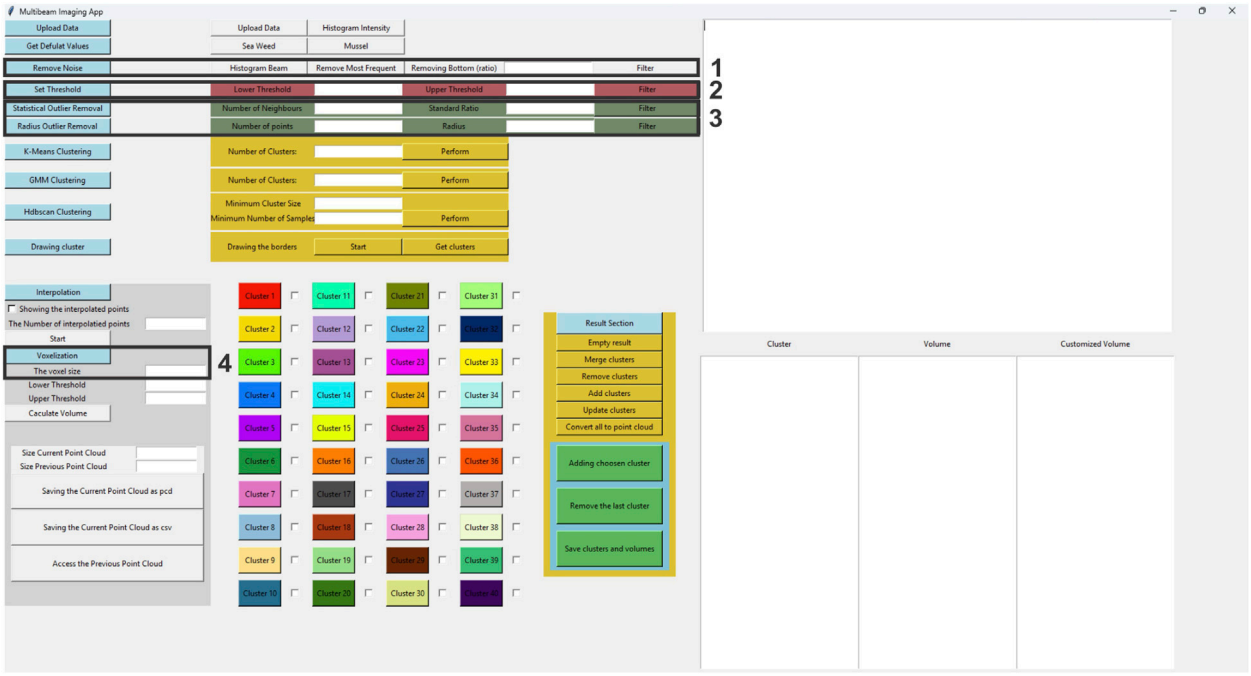

FIGURE 6
Graphical user interface of CloudVolume_multibeam. Highlighted features are noise removal (1), thresholding (2), oultier removal (3) and voxel dimension input (4).

movement due to currents, the location of individual dropper lines may shift between passes, inducing errors. Therefore, data from just one pass are loaded in our case. The goal of CloudVolume_multibeam is to filter the point cloud data file and semi-automatically detect and segment dropper lines, eventually allowing to estimate the volume of the biomass on each dropper line individually (henceforth called "acoustic volume"). In CloudVolume_multibeam, four main steps can be executed: filtering, clustering, interpolation and acoustic volume calculation.

3.2.1 Filtering

The goal of filtering is to remove all data points not related to the aquaculture setup. To achieve this goal, three filtering steps are provided: noise removal, thresholding and outlier removal (Figure 6). The user can choose which steps to apply and in which order.

Noise removal consists of two parts, the first of which is based on the removal of histogram bins with extremely high occurrences, indicating hardware artefacts. Due to unknown reasons, for each ping a large amount of MBWC data points (on average about 27,000) are created by the multibeam echosounder with beam number "32,767". The data points with this beam number are present at the outer edges of each ping echogram (Figure 3) and are artefacts which should be removed. In histograms plotting the amount of occurrences of each beam number, they stand out. Users can delete this artefact by deleting the largest histogram bin (compare Figure 7A versus Figure 7B). In our dataset, this reduces the amount of data points from 24.7 million to nearly 19 million. The second part of noise removal focuses on data close to the minimum slant range, determined by the shortest radial distance between the sonar and the seafloor (Figures 3, 4). The exact position of the first arrival may be slightly wrong due to penetration of the acoustic signal into the seafloor. To counter this effect on the minimum slant range, a user-defined percentage of the water column data, relative to the slant range (Figure 7C), can be deleted to make sure no data affected by sidelobes are retained. We opted for an arbitrary 10% and removed about 2 million data points as a consequence.

The second filtering step is thresholding. Aquaculture installations (in this case bivalves) have higher backscatter values compared to the background (water and suspended sediments), allowing to filter on backscatter values. A lower and upper threshold can be defined, allowing to remove background scatterers as well as anomalously high scatterers remaining after the noise removal step. The values for the thresholds can be obtained by examining the data and identifying which values are associated with the aquaculture setup. If backscatter-calibrated multibeam echosounders would be used, these threshold values would be transferable between studies. In this case, the multibeam echosounder was not calibrated for backscatter intensities, meaning that the applied values are only relevant for this dataset. With this step, you can remove most of the unwanted scatterers in the water column, eliminating over 99% of the data points in our case (using raw backscatter intensity values of 75 and 1750). The resulting point cloud can be seen in Figure 7D.

The third and final filtering step is outlier removal. After thresholding, unwanted data points can still be present within the dataset and may have similar backscatter values as the aquaculture installation. Consequently, they cannot be deleted by thresholding. To delete those data points, both statistical outlier

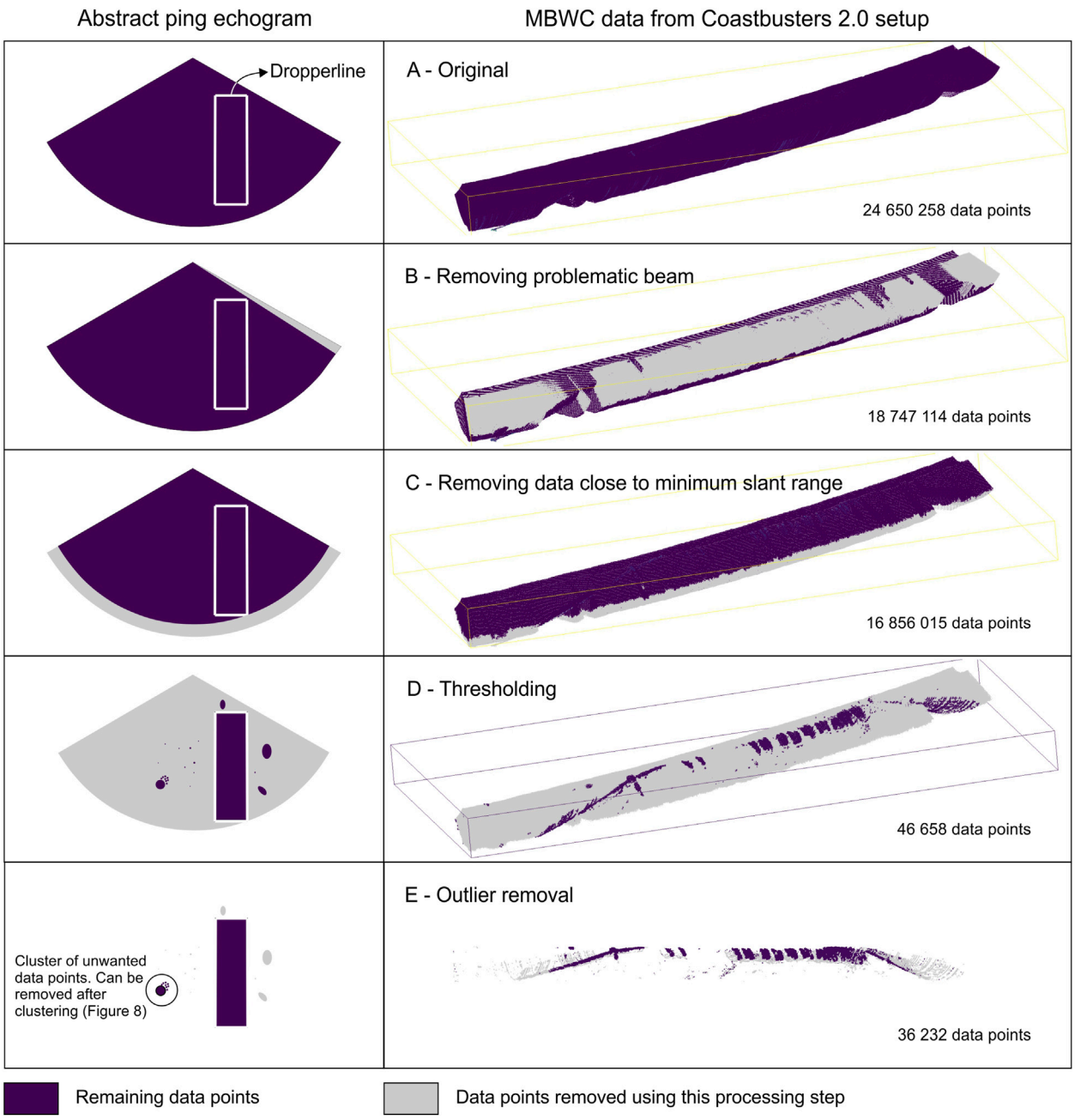

FIGURE 7
Filtering steps applied in CloudVolume_multibeam. **(A)** original, **(B)** removing problematic beam, **(C)** removing data close to the minimum slant range, **(D)** thresholding and **(E)** outlier removal. For each step, an abstract ping echogram (left) and the entire point cloud dataset of the northern longline (right, Figure 5) are displayed. The data points which will be deleted during each filtering step are displayed in grey, while the remaining data points are displayed in purple. In each consecutive filtering step, the data points deleted during the previous step are not displayed anymore: e.g., the grey points in part **(B)** are not displayed anymore in part **(C)**. Finally (part **(E)**), data points related to the dropper lines and some larger clusters remain.

removal and radius outlier removal can be applied to the dataset. Statistical outlier removal deletes data points based on the standard deviation of the distance of a data point to its closest neighbors. If that standard deviation exceeds a predefined value, this data point is removed (Rusu, 2010). Defining the amount of points to be considered for calculating the average distance and the threshold value for the standard deviation can be specified in CloudVolume_multibeam. Radius outlier removal counts the amount of neighboring data points within a certain sphere and if that number is smaller than a threshold, the data point is removed (Szutor and Zichar, 2023). Radius outlier removal requires the definition of the radius and the threshold. Both outlier removal methods can be applied several consecutive times. In our case, another 10,426 data points have been removed by applying the radius outlier removal (at least 200 neighboring points and a threshold radius of 0.5 m)

followed by statistical outlier removal (minimum of 200 neighboring data points and a standard deviation of the average distance of 2).

All three filtering steps can be repeated until as much unwanted data points as possible are removed. Eventually, only data points associated with the aquaculture installations should remain. However, some larger unwanted clusters of data points can still be present (Figure 7E), but can be deleted after clustering (see next section). The result of the filtering steps applied within this study is visualized in Figure 7E.

3.2.2 Clustering

After filtering, a point cloud dataset of the longline and dropperlines remains. To assess the biomass on the individual dropperlines, their volume needs to be obtained and clustering of the data points into separate entities comprising individual dropper lines is necessary. Clustering of data points can be accomplished with three different algorithms using CloudVolume_multibeam, namely K-means clustering, Gaussian Mixed Model clustering and Hdbscan clustering.

The first method is K-means clustering, a relatively simple and low computationally-complex method, which groups points into a predefined number of clusters based on their proximity to centers of intensity (Ikotun et al., 2023). Two metrics can be used to derive possible centers of intensity: the distance between the individual data points or backscatter intensity. CloudVolume_multibeam uses the distance between data points to calculate clusters based on K-means clustering.

The second method is Gaussian Mixture Model (GMM) clustering, which assigns points to a finite number of clusters by considering them as a multi-modal distribution, consisting of a combination of Gaussian distributions with unknown parameters (Takeda and Kimbara, 2022). GMM clustering methods do not require a predefined number of clusters, but in our case the amount of dropper lines is known (they can be counted from the beamstack profile) and can be provided. Be aware that the longline also needs to be considered as a cluster. GMM clustering will divide the data points among the predefined amount of clusters.

The third and final clustering method is Hierarchical Density-Based Spatial Clustering of Applications with Noise (Hdbscan). Hdbscan clustering defines a number of density-based clusters, characterized by high densities of data points, surrounded by low-density areas (generally considered as noise) and organizes these clusters hierarchically (Campello et al., 2020). Hdbscan requires the definition of what should be considered as a dense area and what the minimum numbers of points per clusters should be. The number of clusters cannot be defined.

All clustering methods can be repeated and/or combined until as many dropper lines as possible are classified as individual clusters. Individual clusters can be saved as individual point cloud files and loaded into other applications. Our dataset was divided into clusters using Hdbscan with the following settings: (1) at least 100 data points are needed to be considered a dense area and (2) 100 data points is the minimum cluster size. When applying this clustering method, 22 clusters are obtained (Figure 8A). Several clusters are clearly not dropper lines and can be discarded using the software, leaving just 14 clusters as a result (Figure 8B) of which we aim to calculate their volume. In Figure 8B, you can see that several dropper lines continue to be part of a single cluster. This is mainly because they are located very close to each other and do not have a clear separation in the data. For these dropper lines, manual separation is possible. One of these groups is the red cluster displayed in Figure 8B. A principal component analysis of the x, y and z values is performed and visualized in Figure 8C. In this 2D display, polygons can be drawn around the individual (sub-) clusters to separate them (result in Figure 8D). Performing this manual separation method for all grouped dropper lines will result in the separation of all dropper lines (in our case again clusters), after which volume calculations can be performed on them separately (Figure 8E).

3.2.3 Acoustic volume calculation

Several methods exist to derive the volume of point cloud data, divided into 3 categories (Ling et al., 2024). (1) Slice-based methods slice the data points into individual layers, count the amount of points in each layer and integrate the volume of each layer to estimate the total volume (Zhou et al., 2021). (2) Voxel-based methods divide the three-dimensional space into regular 3D voxel grids and the occupied voxels are counted and multiplied by the voxel volume to obtain the volume of the object (Bienert et al., 2014; Moreno et al., 2020). (3) 3D convex hull methods, constructed using the α-shape method (Edelsbrunner et al., 1983), calculate the volume of an object by summing the positive and negative volumes of triangular prisms projected onto a plane.

We decided to estimate the volume of each dropper line using the voxel-based method. The voxel size (length of the cube's edge in meters) can be specified in CloudVolume_multibeam (Figure 6). The lower the distance between consecutive pings and the lower the inter-sample distance, the smaller the voxel size that can be chosen. This approach requires a point cloud that is dense enough to yield accurate volume estimates. Unfortunately our point cloud is not dense enough due to the relatively large distances between consecutive pings, 16.5 cm on average, and the relatively large inter-sample distance, 10.9 cm on average. Therefore, we densified our point cloud using an interpolation method.

3.2.4 Interpolation

Only 3 to 5 pings (depending on the width of the dropper line) ensonify each dropper line. Although sufficient for 2D (Figure 3) and 3D (Figure 5) visualization, this is insufficient to accurately estimate volumes, the error margin would be too large. Therefore, CloudVolume_multibeam offers the possibility of interpolation.

For each cluster, the interpolation algorithm generates additional points between the point sets of consecutive pings. Each ping is represented as an ordered list of 3D points, preserved exactly as they appear in the input data. The interpolation pairs points from two consecutive pings by their index positions in their respective list, and linearly interpolates their 3D coordinates to create a number of intermediate points. When the two pings contain a different number of points, only pairs up to the length of the shortest list are used. This produces a sequence of interpolated points between the original pings and results in a densified point cloud for each cluster. This in turn decreases the error using the voxel volume estimation method. Figure 9 visualizes the interpolation method outlined above. Linear interpolation is only possible if the input data contains ping number, as this is used by the script to create the ordered lists of 3D points.

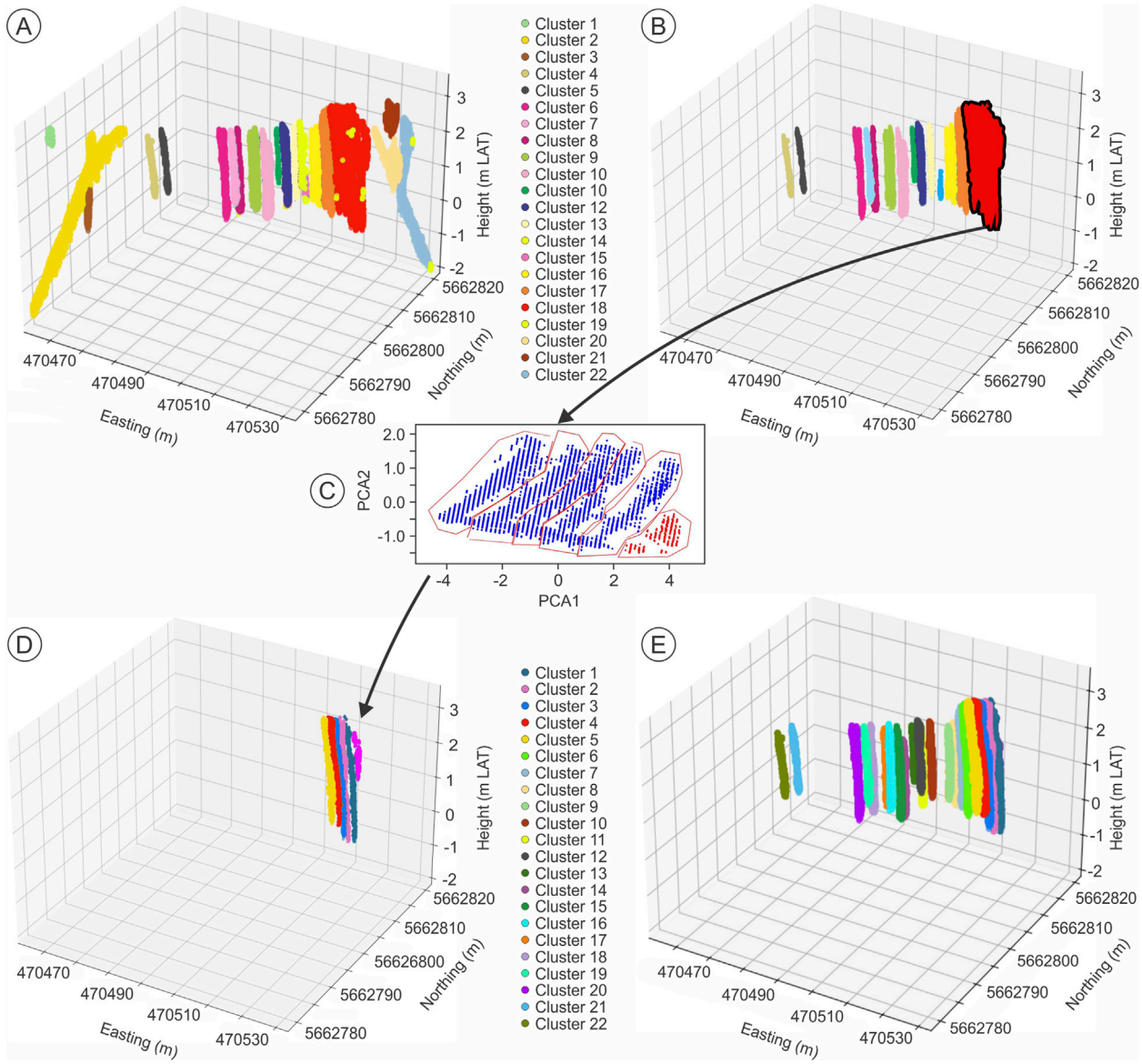

FIGURE 8
Clustering of the point cloud data resulting from the filtering steps. **(A)** 22 clusters are obtained after performing HDBscan (settings in text). **(B)** Selection of a grouped cluster for manual separation. **(C)** The 6 sub-clusters are separated manually by drawing polygons around them. **(D)** Separated sub-clusters after manual clustering. **(E)** Final view of all separated clusters. Their acoustic volumes can be consulted in Table 2. Note that the clusters attributed to the longline were removed.

The amount of interpolations can be specified in CloudVolume_multibeam. In our case, 15 interpolations have been executed.

4 Results and discussion

4.1 Acoustic visualization of aquaculture setups

Two longlines and their individual dropperlines can be discerned on the 3D visualization (Figure 5). Note the different colors of the point data near the bottom of the southern longline (green and blueish colors), which result from higher backscatter values due to their occurrence beyond the minimum slant range. This is a minor fraction of the relevant data points and is mainly because these MBWC data points are close to or on the seafloor, where the minimum slant range is close to the seafloor (Figures 3, 4). Additionally, depending on the distance between the multibeam echosounder and the dropper line and the opening angle of the multibeam, parts of the longline and a fraction of the upper part of the dropper line may not be within the echogram range (Figure 4). The result is the absence of the central part of the longline in the 3D visualization as can be seen on both longlines in Figure 5.

Nevertheless, the 2D and 3D visualizations are powerful tools for aquaculture managers to assess the status of their longlines since effective and frequent inspections are crucial for understanding the

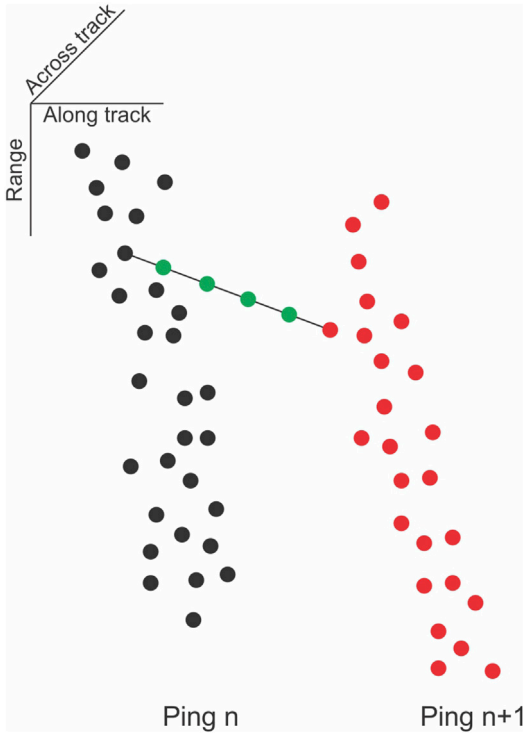

FIGURE 9
Interpolation method used within CloudVolume_multibeam. In this figure, four intermediate points (green dots) are created between pairs of points within ping N (black dots) and ping N+1 (red dots). The same interpolation is executed between all pairs of points between consecutive pings of each cluster.

structural health of aquaculture setups and being able to assess their production capacity. Usually, the ropes of the longline system are lifted to measure their extent and conduct sampling at the same time (Arantzamendi et al., 2024; Goedefroo et al., 2022). However, this technique is rather time consuming and costly, given the large vessel and sufficient crew that needs to be foreseen. Moreover, calm sea conditions and low currents are required to perform these activities and hoisting and handling of the lines leads to mussels getting damaged or falling off the lines, altering the biomass on the lines. Alternatively, under-water video footage can be difficult to obtain given the relatively high turbidity within the Belgian part of the North Sea (Baeye et al., 2011; Fettweis et al., 2019). Acoustic monitoring of the longline system, using MBWC data, is a promising technique which dismisses several of the shortcomings of the previously mentioned methods. Acquisition of MBWC data does not require larger vessels and adequate crew (even small RHIB's can be used; Figure 2), is far less affected by high turbidity and the longline does not need to be physically manipulated, preventing damage to the system or loss of mussels during inspection. This study proves that MBWC data can visualize the longline in sufficient detail (Figure 5).

Other types of acoustic data can also be used to visualize aquaculture longlines. A study by Peck et al. (2024), conducted within the framework of the Coastbusters 2.0 project, showed that also sidescan sonar imagery, acquired using an autonomous underwater vehicle (AUV), holds potential to assess the status of the same longline system as the one within this study. The use of MBWC data however has two main advantages compared to sidescan sonar imagery. First, point cloud data can be generated from MBWC data, allowing to visualize the setup in 3D, compared to the 2D images of the sidescan sonar. Second, volume estimates are possible with MBWC data since all data is georeferenced and in 3D. Conversely, the sidescan sonar imagery of Peck et al. (2024) has two main advantages compared to the MBWC data in this study. First, the sidescan sonar imagery has a higher range resolution (due to its operating frequencies of 455 and 900 kHz) and second, the sidescan sonar data allow the entire longline to be visualized at once due to the 45° opening angles (3 dB angle), the installation angle of both SSS transducers at 57° and because the AUV dove below the longline (Peck et al., 2024). In our case, the upper parts of the longline were not entirely ensonified due to their position outside the acoustic swath plane (Figures 3, 5). Using multibeam echosounders with higher frequencies (e.g., 700 kHz) could help resolve the lower range resolution of the MBWC data compared to sidescan sonar data, while tilting the multibeam sonar towards the longline, either mechanically or electronically, could help visualizing the entire longline at once, eliminating the disadvantages of multibeam data compared to sidescan sonar data in the future.

4.2 Assessment of longline setup

Within the Coastbusters 2.0 project, seasonal dropper line inspection surveys have been undertaken to weigh and measure (circumference of top and bottom) selected dropper lines as well as to check their integrity (Leinung, 2023; Figure 10). Due to the time-consuming and costly nature of the surveys, not all dropper lines could be lifted and visually assessed each time, resulting in an incomplete view of the setup, often extrapolated using assumptions (Figure 10). For aquaculture farmers, who are using similar methods, this may result in under- or overestimations of the biomass. MBWC data resolves this issue, as a complete visualization can be achieved within minutes. BeamworX NavAQ software for MBES data acquisition includes a beamstack profile visualization of water column data (2D display, comparable to Figure 3), allowing to assess the status of the longline immediately by the surveyor. For detailed 3D inspection and acoustic volume estimations, processing of the data needs to take place, which has to be conducted in the office. This can be done using CloudVolume_multibeam.

Comparison of the MBWC data to the dropper line inspection survey data closest in time before and after multibeam data acquisition (respectively 13/09/2021 and 14/12/2021) reveals some interesting findings:

1. Some of the dropper lines (3, 6 and 9) which were observed to be lost in December 2021 were already lost at the time of multibeam acquisition (October 2021; Figure 10).
2. The SW side of the longline (dropper lines 37, 38 and 39) was not checked during the December dropper line inspection survey and was assumed intact. However, the MBWC data clearly indicate just 2 out of 3 assumed dropper lines are present. Based on the distance between them, dropper line 38 is

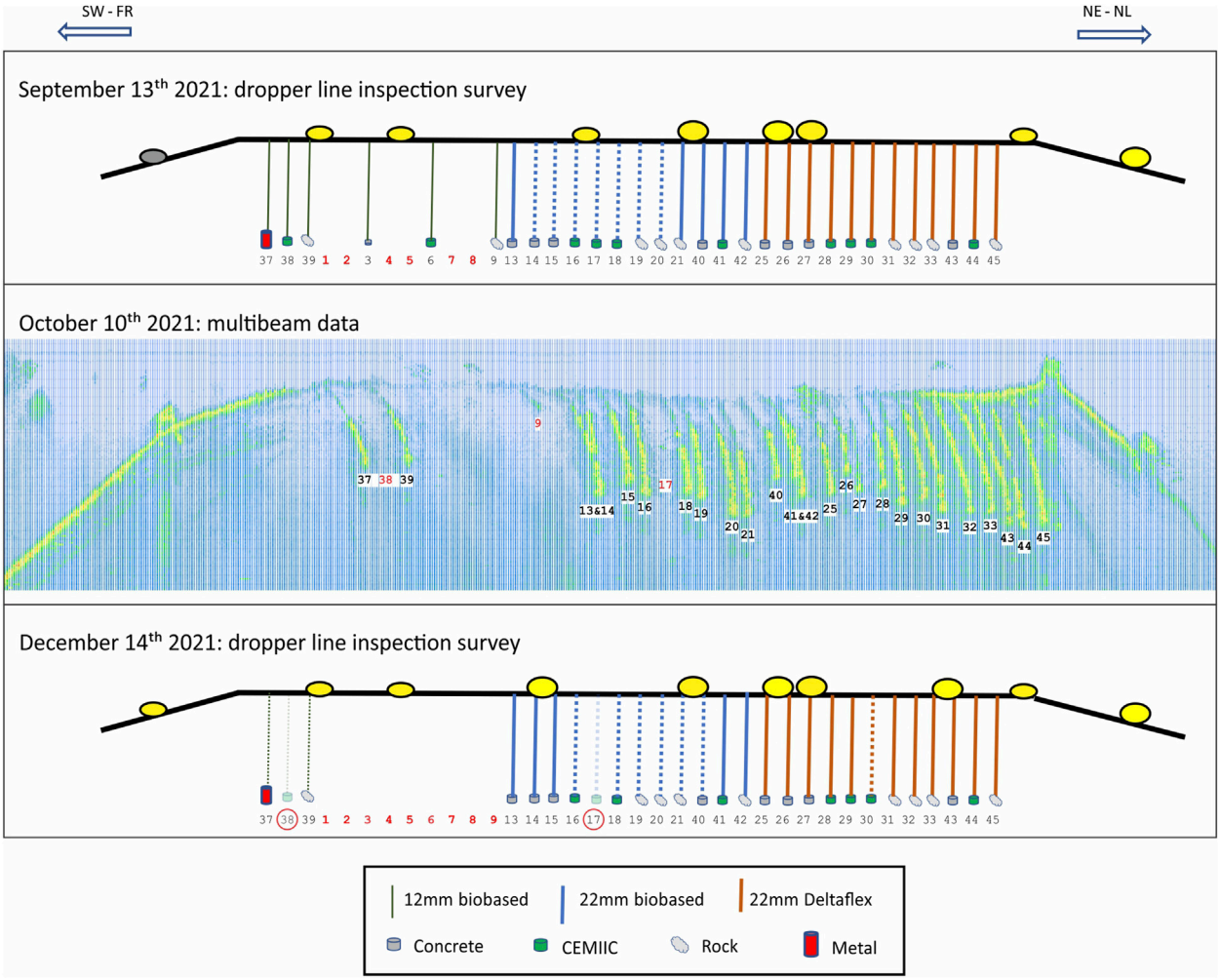

FIGURE 10
Comparison of the dropper line inspection survey data before (13/09/2021) and after (14/12/2021) acquisition of the MBWC data (10/10/2021). Dropper lines not inspected, but assumed intact are displayed as dashed lines. Lost dropper lines have their numbers displayed in red. On 14/12/2021, dropper line 38 and 17 (circled in red) were assumed intact, but MBWC data indicate they were actually already lost. The colors of the dropper lines indicate their fabric, while their bases either consist of concrete, rock, metal or cemIIc (Narimane et al., 2020).

labelled as missing (Figure 10). In addition, dropper 17 was not lifted in September or December and was assumed intact by the scientists conducting the dropper line inspection surveys. However, dropper 17 is not visible within the MBWC data, indicating it was most likely already lost before the multibeam survey of October.

These examples indicate one of the main advantages of MBWC data compared to the traditional methods: a complete overview of the longline is obtained within minutes and no assumptions are necessary. Without the MBWC data, the fact that the dropper lines mentioned above are missing could only be observed in December 2021 or could even continue to be assumed intact if they are not lifted or counted properly in the following dropper line inspection surveys. Also entanglements of dropper lines are immediately visible (e.g., dropper lines 13 and 14; Figure 10). In essence, MBWC data provides a much more accurate overview of the status of the longline setup, compared to manual inspection surveys.

4.3 Acoustic volume estimates

After interpolating 15 times between consecutive pings and using voxels with edges of 5 cm, the obtained acoustic volumes are between 0.21 m^3 and 1.21 m^3 (Table 2). These are realistic values given the circumferences specified in Table 1 and the length of the dropper lines at the time of installation, which was 3 m. Since, exact volume measurements of the biomass on the dropper lines are not available, the determination of an error margin for the applied method is not possible though.

A number of options could be explored to improve the volume estimations. These include:

4.3.1 Reduce sidelobe interference

All data beyond the minimum slant range have been deleted for volume estimations since thresholding is based on backscatter values and all backscatter values beyond the minimum slant range are affected by sidelobe interference (Hughes Clarke, 2006; Urban et al., 2017; Liu et al., 2019; Schimel et al., 2020). Several studies and scripts

TABLE 2 Acoustic volumes, using voxels with edges of 5 cm, of the identified dropper lines. Cluster numbers refer to the numbering in Figure 8, while dropper line numbers refer to the labels in Figure 10.

Dropper line number	Cluster number	Acoustic volume (m^3)
45	1	1,21
44	2	1,06
43	3	0,92
33	4	0,99
32	5	0,87
31	6	0,91
30	7	0,90
29	8	0,79
28	9	0,68
26	10	0,92
25	11	0,73
41&42	12	0,64
40	13	0,75
21	14	0,57
20	15	0,54
19	16	0,49
18	17	0,41
16	18	0,60
15	19	0,52
13&14	20	0,30
39	21	0,21
37	22	0,28

already exist to reduce the effect of sidelobe interference (Nau et al., 2025; Schimel et al., 2020; Liu et al., 2019), but none of them completely suppress or filter the sidelobe signal. This means that although the sidelobe effect will be reduced, the backscatter values above and beyond the minimum slant range will still be slightly different and thresholding based on backscatter values will still be affected. Range-dependent threshold levels or object-detection algorithms could be explored to improve the detection of the dropper lines within the MBWC-generated point cloud data.

4.3.2 Improve the data density

Theoretically, improving the acoustic volume estimates can be achieved by improving the data density in all 3 dimensions; along-track (distance between consecutive swath planes), across-track (inter-beam distance) and range (inter-sample distance). This would enable to reduce the amount of interpolations, or even completely render them superfluous, allowing to use smaller voxel sizes, eventually yielding more accurate acoustic volume estimates. The along-track data density can be improved by using multibeam echosounders which allow to record MBWC data at higher ping rates, without compromising the inter-sample and inter-beam distance. Since the dropper lines are usually in the range between 1 and 5 m (Figure 3), theoretical ping rates of 150 Hz could be used. However, most modern multibeam echosounders have a maximum ping rate of 50 Hz or 60 Hz (e.g., Kongsberg, 2025; Norbit, 2025; R2sonic, 2025; Teledyne Reson, 2025), setting a practical threshold. The across-track data density can be improved by generating more beams and reducing the swath opening angle as much as possible. The inter-sample distance can be improved by using multibeam echosounders with a higher sampling frequency. Finally, using multibeam echosounders with smaller beamwidths will improve target separability in the angular dimension (across-track). This will enable to define the edges of the dropper lines in the MBWC data better and will improve the acoustic volume estimates as well.

4.3.3 Adopting alternative volume estimation methods

The approach used in this study is comparable to Nau et al. (2025), where the volume of kelp was calculated based on multiplying the average height of kelp above the seafloor with the surface of the grid resolution. However, alternative methods to calculate volumes based on point cloud data could be explored to improve the volume estimations. Possible methods include the mentioned slice-based or 3D convex hull-based methods (Ling et al., 2024). This inherently involves comparing the acoustic volumes obtained using MBWC data to independent volume data of the biomass on the dropper lines, allowing to derive the error margin of the method. Since actual volumes of the biomass on the dropper lines are not available, error margins cannot be determined and volume methods not compared. Future projects should focus on obtaining these independent, actual volumes of the biomass on the dropper lines.

5 Conclusion

This paper demonstrates that aquaculture longline systems can be monitored using MBWC data and that acoustic volume assessments of the biomass on individual dropper lines can be obtained. Using the CloudVolume_multibeam software, one can filter the data, cluster the dropper lines, interpolate data points if needed and perform acoustic volume estimations using voxels.

Since mussel aquaculture accounts for about 94% of the world's mussel production (Avdelas et al., 2021), MBWC data holds a huge potential for process optimization and profit increases. MBWC data provides aquaculture managers with a novel tool, based on an already-existing and widely-distributed multibeam technology. Indeed, multibeam echosounders are installed on many research and industrial vessels and can be mounted on small workboats, operated by a 2-person crew. The data can be acquired in a matter of minutes (depending on the vessel speed and the length of the longline system) and immediate assessments can be made onboard with recent acquisition software. By using the novel CloudVolume_multibeam software, acoustic volume estimation can be performed, providing aquaculture managers with a tool to assess the biomass of the setup. Future improvements and cost-reducing steps include the usage of unmanned surface or

autonomous underwater vehicles for the acquisition of the MBWC data, improved filtering and clustering steps within CloudVolume_multibeam and more precise acoustic volume estimations.

Data availability statement

The raw data supporting the conclusions of this article will be made available by the authors, without undue reservation.

Ethics statement

Written informed consent was obtained from the individual(s) for the publication of any potentially identifiable images or data included in this article.

Author contributions

TV: Conceptualization, Data curation, Formal Analysis, Investigation, Methodology, Resources, Software, Supervision, Validation, Visualization, Writing – original draft, Writing – review and editing. SL: Methodology, Software, Writing – review and editing. KL: Investigation, Project administration, Resources, Validation, Writing – review and editing. AS: Data curation, Investigation, Writing – review and editing. GV: Data curation, Investigation, Writing – review and editing. TS: Funding acquisition, Project administration, Writing – review and editing. IM: Funding acquisition, Project administration, Writing – review and editing.

Funding

The author(s) declared that financial support was received for this work and/or its publication. The authors wish to thank VLAIO and the Blue Cluster for providing funds for the Coastbusters 2.0 project (HBC.2019.0037) and Horizon Europe to provide funds for the ULTFARMS project (grant agreement 101093888).

Acknowledgements

All project partners of both projects are acknowledged for their part in the success of the projects. A sincere thanks to Nore Praet and Jan Vermaut for their help in acquiring the MBWC data used within this study as well as to Koen and Frank from Brevisco for their help at sea during the dropper line inspection surveys. Insightful comments were received by two reviewers and the editor, improving the readability and accuracy of the manuscript.

Conflict of interest

Author TS was employed by DEME.

The remaining author(s) declared that this work was conducted in the absence of any commercial or financial relationships that could be construed as a potential conflict of interest.

Generative AI statement

The author(s) declared that generative AI was not used in the creation of this manuscript.

Any alternative text (alt text) provided alongside figures in this article has been generated by Frontiers with the support of artificial intelligence and reasonable efforts have been made to ensure accuracy, including review by the authors wherever possible. If you identify any issues, please contact us.

Publisher's note

References

Ali, A., Abdullah, M. R., Safuan, C. D. M., Afiq-Firdaus, A. M., Bachok, Z., Akhir, M. F. M., et al. (2022). Side-scan sonar coupled with scuba diving observation for enhanced monitoring of benthic artificial reefs along the Coast of Terengganu, peninsular Malaysia. *J. Mar. Sci. Eng.* 10, 1309. doi:10.3390/jmse10091309

Arantzamendi, L., Andrés, M., Suárez, M. J., Van Der Schueren, L., and Aguinaga, M. (2024). Assessing the mechanical properties of biobased versus fossil-based ropes and their impact on the productivity and quality of mussel (Mytilus galloprovincialis) in longline aquaculture: toward decarbonization. *Aquaculture* 588, 740919. doi:10.1016/j.aquaculture.2024.740919

Avdelas, L., Avdic-Mravlje, E., Borges Marques, A. C., Cano, S., Capelle, J. J., Carvalho, N., et al. (2021). The decline of mussel aquaculture in the european union: causes, economic impacts and opportunities. *Rev. Aquac.* 13, 91–118. doi:10.1111/raq.12465

Baeye, M., Fettweis, M., Voulgaris, G., and Van Lancker, V. (2011). Sediment mobility in response to tidal and wind-driven flows along the Belgian inner shelf, southern north sea. *Ocean. Dyn.* 61, 611–622. doi:10.1007/s10236-010-0370-7

Bao, J., Li, D., Qiao, X., and Rauschenbach, T. (2020). Integrated navigation for autonomous underwater vehicles in aquaculture: a review. *Inf. Process. Agric.* 7, 139–151. doi:10.1016/j.inpa.2019.04.003

Bienert, A., Hess, C., Maas, H. G., and Von Oheimb, G. (2014). A voxel-based technique to estimate the volume of trees from terrestrial laser scanner data. *Int. Arch. Photogramm. Remote Sens. Spat. Inf. Sci.* XL-5, 101–106. doi:10.5194/isprsarchives-xl-5-101-2014

Boulenger, A., Lanza-Arroyo, P., Langedock, K., Semeraro, A., and Van Hoey, G. (2024). Nature-based solutions for coastal protection in sheltered and exposed coastal waters: integrated monitoring program for baseline ecological structure and functioning assessment. *Environ. Monit. Assess.* 196, 316. doi:10.1007/s10661-024-12480-x

Brehmer, P., Gerlotto, F., Guillard, J., Sanguinède, F., Guénnegan, Y., and Buestel, D. (2003). New applications of hydroacoustic methods for monitoring shallow water aquatic ecosystems: the case of mussel culture grounds. *Aquat. Living Resour.* 16, 333–338. doi:10.1016/s0990-7440(03)00042-1

Brehmer, P., Vercelli, C., Gerlotto, F., Sanguinède, F., Pichot, Y., Guennégan, Y., et al. (2006). Multibeam sonar detection of suspended mussel culture grounds in the open sea: direct observation methods for management purposes. *Aquaculture* 252, 234–241. doi:10.1016/j.aquaculture.2005.06.035

Campello, R. J. G. B., Kröger, P., Sander, J., and Zimek, A. (2020). Density-based clustering. *WIREs Data Min. Knowl. Discov.* 10, e1343. doi:10.1002/widm.1343

COASTBUSTERS2.0 (2023). Ecosystem based coastal management. Available online at: https://www.blauwecluster.be/sites/default/files/2023-10/coa-23.09-eindrapport-v4.3_0.pdf (Accessed November 13, 2025).

Colbo, K., Ross, T., Brown, C., and Weber, T. (2014). A review of oceanographic applications of water column data from multibeam echosounders. *Estuar. Coast. Shelf Sci.* 145, 41–56. doi:10.1016/j.ecss.2014.04.002

Edelsbrunner, H., Kirkpatrick, D., and Seidel, R. (1983). On the shape of a set of points in the plane. *IEEE Trans. Inf. Theory* 29, 551–559. doi:10.1109/tit.1983.1056714

English, G., Lawrence, M. J., Mckindsey, C. W., Lacoursière-Roussel, A., Bergeron, H., Gauthier, S., et al. (2024). A review of data collection methods used to monitor the associations of wild species with marine aquaculture sites. *Rev. Aquac.* 16, 1160–1185. doi:10.1111/raq.12890

FAO (2020). *The state of world fisheries and aquaculture 2020. Sustainability in action*. Rome, Italy: FAO.

FAO (2022). *The state of world fisheries and aquaculture 2022. Towards blue transformation*. Rome, Italy: FAO.

Fettweis, M., Riethmüller, R., Verney, R., Becker, M., Backers, J., Baeye, M., et al. (2019). Uncertainties associated with *in situ* high-frequency long-term observations of suspended particulate matter concentration using optical and acoustic sensors. *Prog. Oceanogr.* 178, 102162. doi:10.1016/j.pocean.2019.102162

Fromant, G., Le Dantec, N., Perrot, Y., Floc'h, F., Lebourges-Dhaussy, A., and Delacourt, C. (2021). Suspended sediment concentration field quantified from a calibrated MultiBeam EchoSounder. *Appl. Acoust.* 180, 108107. doi:10.1016/j.apacoust.2021.108107

Goedefroo, N., Benham, P., Debusschere, E., Deneudt, K., Mascart, T., Semeraro, A., et al. (2022). Nature-based solutions in a sandy foreshore: a biological assessment of a longline mussel aquaculture technique to establish subtidal reefs. *Ecol. Eng.* 185, 106807. doi:10.1016/j.ecoleng.2022.106807

Higgs, B., Mountjoy, J. J., Crutchley, G. J., Townend, J., Ladroit, Y., Greinert, J., et al. (2019). Seep-bubble characteristics and gas flow rates from a shallow-water, high-density seep field on the shelf-to-slope transition of the Hikurangi subduction margin. *Mar. Geol.* 417, 105985. doi:10.1016/j.margeo.2019.105985

Hughes Clarke, J. E. (2006). Applications of multibeam water column imaging for hydrographic survey.

Ikotun, A. M., Ezugwu, A. E., Abualigah, L., Abuhaija, B., and Heming, J. (2023). K-means clustering algorithms: a comprehensive review, variants analysis, and advances in the era of big data. *Inf. Sci.* 622, 178–210. doi:10.1016/j.ins.2022.11.139

Innangi, S., Bonanno, A., Tonielli, R., Gerlotto, F., Innangi, M., and Mazzola, S. (2016). High resolution 3-D shapes of fish schools: a new method to use the water column backscatter from hydrographic MultiBeam echo sounders. *Appl. Acoust.* 111, 148–160. doi:10.1016/j.apacoust.2016.04.017

Kongsberg (2025). EM2042 multibeam echosounder. Available online at: https://www.kongsberg.com/discovery/seafloor-mapping/em/em2042/ (Accessed November 24, 2025).

Lashkari, S., and Vandorpe, T. (2025). CloudVolume_multibeam. Available online at: https://github.com/vlizBE/CloudVolume_multibeam?tab=readme-ov-file.

Leinung, C. (2023). *Application of aquaculture techniques to create biogenic mussels reefs as a nature-based solution for coastal stabilization: evaluating 6 years of the coastbusters projects*. MSc, Ghent: Ghent University.

Li, D., Du, Z., Wang, Q., Wang, J., and Du, L. (2024). Recent advances in acoustic technology for aquaculture: a review. *Rev. Aquac.* 16, 357–381. doi:10.1111/raq.12842

Ling, Y., Zhao, R., Shen, Y., Li, D., Jin, J., and Liu, J. (2024). DIVESPOT: depth integrated volume estimation of pile of things based on point cloud. *arXiv Preprint arXiv:2407.05415*. doi:10.48550/arXiv.2407.05415

Liu, H., Yang, F., Zheng, S., Li, Q., Li, D., and Zhu, H. (2019). A method of sidelobe effect suppression for multibeam water column images based on an adaptive soft threshold. *Appl. Acoust.* 148, 467–475. doi:10.1016/j.apacoust.2019.01.006

Lowry, M. B., Glasby, T. M., Boys, C. A., Folpp, H., Suthers, I., and Gregson, M. (2014). Response of fish communities to the deployment of estuarine artificial reefs for fisheries enhancement. *Fish. Manag. Ecol.* 21, 42–56. doi:10.1111/fme.12048

Moreno, H., Valero, C., Bengochea-Guevara, J. M., Ribeiro, Á., Garrido-Izard, M., and Andújar, D. (2020). On-Ground vineyard reconstruction using a LiDAR-Based automated system. *Sensors* 20, 1102. doi:10.3390/s20041102

Narimane, Z., Zedira, H., Castro-Gomez, J. P., Bezzazi, B., Talah, A., and Benbouras, M. A. (2020). Evolution of durability and mechanical properties of ordinary portland cement concretes in sulphates attack. *Eng. Rev.* 40, 32–41. doi:10.30765/er.40.3.04

Nau, A. W., Lucieer, V., Schimel, A. C. G., Kunnath, H., Ladroit, Y., and Martin, T. (2025). Advanced detection and classification of kelp habitats using multibeam echosounder water column point cloud data. *Remote Sens.* 17, 449. doi:10.3390/rs17030449

Naylor, R. L., Hardy, R. W., Buschmann, A. H., Bush, S. R., Cao, L., Klinger, D. H., et al. (2021). A 20-year retrospective review of global aquaculture. *Nature* 591, 551–563. doi:10.1038/s41586-021-03308-6

Norbit (2025). *Multibeam sonars with ultimate flexibility*. Available online at: https://norbit.com/product/norbit-winghead-i77h/ (Accessed November 24, 2025).

Peck, C. J., Langedock, K., Boone, W., Fourie, F., Moulaert, I., Semeraro, A., et al. (2024). The use of autonomous underwater vehicles for monitoring aquaculture setups in a high-energy shallow water environment: case study Belgian north sea. *Front. Mar. Sci.* 11, 1386267. doi:10.3389/fmars.2024.1386267

Praet, N., Collart, T., Ollevier, A., Roche, M., Degrendele, K., De Rijcke, M., et al. (2023). The potential of multibeam sonars as 3D turbidity and SPM monitoring tool in the north sea. *Remote Sens.* 15, 4918. doi:10.3390/rs15204918

R2sonic (2025). Sonic® 2026-V Multibeam Echosounder. Available online at: https://r2sonic.com/products/sonic-2026/(Accessed November 24, 2025).

Rusu, R. B. (2010). Semantic 3D object maps for everyday manipulation in human living environments. *KI - Künstliche Intell.* 24, 345–348. doi:10.1007/s13218-010-0059-6

Schimel, A. C. G., Brown, C. J., and Ierodiaconou, D. (2020). Automated filtering of multibeam water-column data to detect relative abundance of giant kelp (Macrocystis pyrifera). *Remote Sens.* 12, 1371. doi:10.3390/rs12091371

Szutor, P., and Zichar, M. (2023). Fast radius outlier filter variant for large point clouds. *Data* 8, 149. doi:10.3390/data8100149

Takeda, K., and Kimbara, K. (2022). Development of estimating algorithm for biodegradation of chemicals using clustering and learning algorithm. *Comput. Aided Chem. Eng.* doi:10.1016/B978-0-323-85159-6.50288-8

Teledyne Reson (2025). SeaBat T50 extended range. Available online at: https://www.teledynemarine.com/brands/reson/seabat-t50-extended-range (Accessed November 24, 2025).

Trenkel, V. M., Mazauric, V., and Berger, L. (2008). The new fisheries multibeam echosounder ME70: description and expected contribution to fisheries research. *ICES J. Mar. Sci.* 65, 645–655. doi:10.1093/icesjms/fsn051

Urban, P., Köser, K., and Greinert, J. (2017). Processing of multibeam water column image data for automated bubble/seep detection and repeated mapping. *Limnol. Oceanogr. Methods* 15, 1–21. doi:10.1002/lom3.10138

Zhou, H., Zhang, J., Ge, L., Yu, X., Wang, Y., and Zhang, C. (2021). Research on volume prediction of single tree canopy based on three-dimensional (3D) LiDAR and clustering segmentation. *Int. J. Remote Sens.* 42, 738–755. doi:10.1080/01431161.2020.1811917